Zirconia doped barium titanate induced electroactive polymorph in PVDF-HFP: high energy density and dielectric properties

2014 Mater. Res. Express 1 045301

Materials Research
Express

Zirconia doped barium titanate induced electroactive β polymorph in PVDF-HFP: high energy density and dielectric properties

Maya Sharma[1], **S Ranganatha**[2], **Ajay Kumar Kalyani**[2], **Rajeev Ranjan**[2], **Giridhar Madras**[1] **and Suryasarathi Bose**[2]
[1] Center for Nano Science and Engineering, Indian Institute of Science, Bangalore-560012, India
[2] Department of Materials Engineering, Indian Institute of Science, Bangalore-560012, India
E-mail: sbose@materials.iisc.ernet.in

Received 17 June 2014
Accepted for publication 9 September 2014
Published 3 October 2014
Materials Research Express **1** (2014) 045301
doi:10.1088/2053-1591/1/4/045301

Abstract

Zirconium-doped barium titanate (BZT-08, $Ba(Ti_{0.92}\ Zr_{0.08})O_3$) particles were synthesized and PVDF-HFP-based composites were prepared by melt mixing to design materials with tunable dielectric and ferroelectric properties. Composites of PVDF-HFP and barium titanate (BT) particles were also prepared to realize the exceptional properties associated with the BZT-08-like stabilization of two ferroelectric phases, i.e. tetragonal and orthorhombic at room temperature. To facilitate the uniform dispersion and interfacial adhesion with the matrix, the particles were modified with (3-aminopropyl) triethoxysilane. The dependence of the dielectric and ferroelectric properties of the as-prepared composites were systematically investigated in this study with respect to a wide range of frequencies. The composites with BZT-08 exhibited the significantly high dielectric permittivity of ca. 26 (at 100 Hz) and a high energy density (2.7 J cm^{-3} measured on 100 μm thick film) at room temperature with respect to the control PVDF-HFP and PVDF-HFP/BT composites. Interestingly, the BZT-08 particles facilitated the electroactive β polymorph in the PVDF-HFP and enhanced polarization in the composites, leading to improved ferroelectric properties in the composites.

Keywords: PVDF-HFP, ceramic particles, energy density

Introduction

In the past decade, there have been remarkable efforts to unite the high ferroelectric properties and high dielectric permittivity of ceramics with the flexibility and ease of processing polymeric materials. Polymeric composites with tunable dielectric and ferroelectric properties are in great demand for various practical applications such as flexible ferroelectric random access memory, electromechanical transducers, artificial muscles, etc Materials with a high dielectric constant and low dielectric loss are in great demand; however, realizing these properties in a single material still remains an open challenge. For instance, ceramic materials such as $BaTiO_3$ (barium titanate, BT) have a high dielectric constant [1, 7, 13]. However, their low breakdown strength restricts their use in high field applications. On the other hand, polymers have a high electrical breakdown strength but very low dielectric permittivity [15, 24]. The idea of ceramic-based polymer composites thus stem from the unique combination of properties from ceramics and polymers [8, 16, 17].

Composites of PVDF and BT have been widely studied in the past. For instance, the breakdown strength of 250 kV mm^{-1} and the high polarization of 3.5 $\mu C\ cm^{-2}$ was realized at 4 and 7 vol% BT particles, respectively, in PVDF. Such a unique combination of properties can be realized if the particles are well dispersed in the polymer matrix [19]. The latter can be obtained by tailoring the surface of the particles, which in turn can facilitate the interfacial adhesion with the matrix polymer. The peculiar dielectric properties of PVDF stem from its crystalline phase as it exhibits aligned C-F dipoles [4, 21]. However, the uniform dispersion of the ceramic particles remains a challenge due to the poor surface free energy of PVDF. In this context, phosphonic acid ligands and other surface modifiers, such as silane and titanate coupling agents, are frequently used to modify the surface of the ceramic particles [2, 3, 6, 9, 12]. The resulting composites showed high permittivity with respect to the unmodified composites and demonstrated the key role of surface modification in realizing the right set of properties.

BT undergoes three structural transitions, namely cubic-tetragonal, tetragonal-orthorhombic and orthorhombic-rhombohedra at $T_{C\text{-}T} \sim 120\,°C$, $T_{T\text{-}O} \sim 5\,°C$ and $T_{O\text{-}R} \sim -90\,°C$, respectively. It is envisaged that the piezoelectric coefficient can be enhanced by tuning the polymorphic transitions close to room temperature. Since the tetragonal-orthorhombic transition occurs at ~5 °C for BT, only dopants that can raise this transition temperature can increase the piezoelectric properties. It is known that zirconia (Zr) substitution in BT increases the tetragonal-orthorhombic and the orthorhombic-rhombohedra transition temperature. Hence, Zr-modification can improve the piezoelectric properties of BT due to the stabilization of two ferroelectric phases, i.e. tetragonal and orthorhombic [10, 11]. Hence, this work systematically investigates the effect of zirconium (Zr)-modified BT particles (BZT-08, $Ba(Ti_{0.92}\,Zr_{0.08})O_3$) in the PVDF-HFP matrix on the dielectric permittivity and ferroelectric properties. At a given load (16 vol%), composites of PVDF-HFP/BT were also compared to understand the key role of BZT-08 in improving the dielectric and energy density. As mentioned, the surface modification of the particles is key to realizing the unique combination of properties; hence, both the BT and BZT-08 particles were modified with (3-aminopropyl) triethoxysilane to enhance their dispersion in PVDF. The ferroelectric properties of the composites were also evaluated.

Materials and methods

Synthesis and modification of particles

$Ba(Ti_{(1-x)}Zr_x)O_3$ ($x = 0$ for BT and $x = 0.08$ for BZT-08) was prepared by a conventional solid state route[17]. The analytical grade reagents of $BaCO_3$, TiO_2 and ZrO_2 were thoroughly mixed in

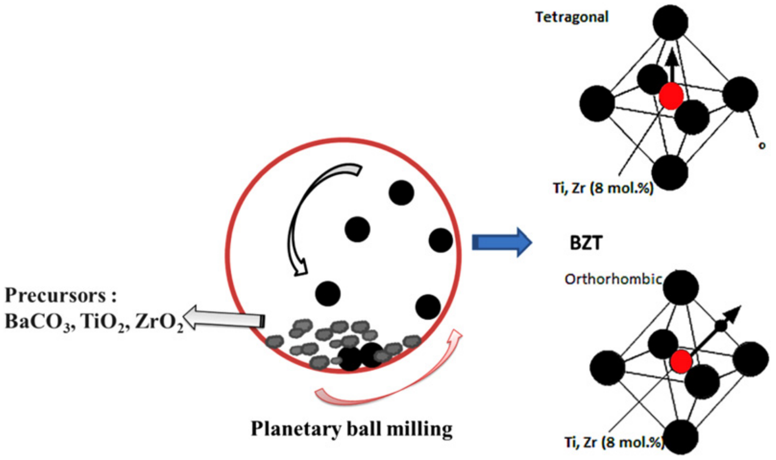

Scheme 1. A cartoon illustrating the ball milling preparation procedure for calcined BZT powder.

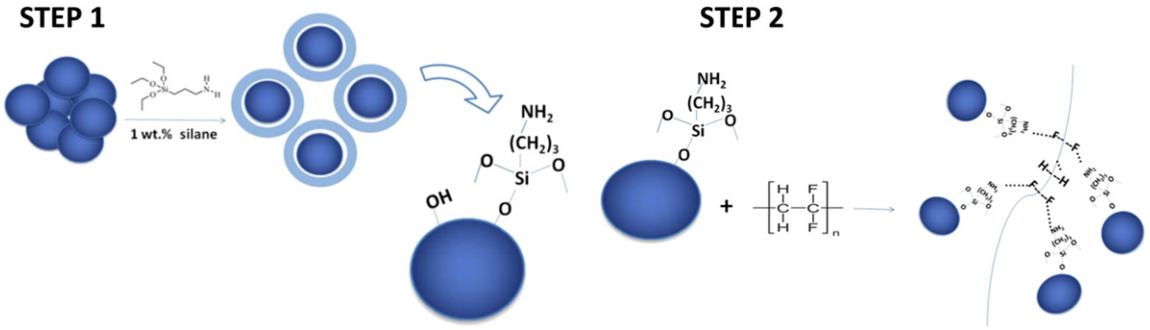

Scheme 2. The stepwise modification route adopted to modify the particles with (3-aminopropyl) triethoxysilane (APTS) (step 1) and the possible interaction of the modified particles with PVDF-HFP (in step 2).

a planetary ball mill (P5, Fritch) for about 10 – 12 h (see scheme 1). After milling, the powders were dried and then heated at 1100 °C for 4 h. Both the BT and BZT-08 particles were chemically modified by (3-aminopropyl) triethoxysilane (APTS) to facilitate uniform dispersion in the PVDF-HFP. The particles were initially dispersed in ethanol and shear mixed for 45 min at 15 000 rpm. 1 wt.% of APTS was added to the mixture and subjected to magnetic stirring for 2 h. These particles were then filtered and washed with ethanol to remove the excess of silane, followed by vacuum drying (see scheme 2).

Preparation of composites

PVDF-HFP ($M_w = 455\,000$) was obtained from Sigma-Aldrich. The PVDF-HFP/BT and PVDF-HFP/BZT-08 composites with 16 vol% particles were prepared by melt mixing, which is an industrially viable route, using a Minilab II HAAKE extruder CTW5 (7cc) at 220 °C with a rotational speed of 60 rpm for 20 min The mixing was performed under an N_2 atmosphere to prevent oxidative degradation. The samples were pre-dried at 80 °C in a vacuum oven for at least 24 h prior to processing. The melt-mixed samples were subsequently compression-molded into thin films using a lab scale hydraulic press.

Characterization

The WXRD patterns were recorded using a PANalytical X'pert Pro to study the structural changes in the PVDF-HFP. The scans were obtained at 40 keV using Cu Kα radiation with a wavelength of 1.54 Å. The Fourier transform infrared (FTIR) spectra of the composites were recorded on a Perkin–Elmer spectrometer GX. The dielectric measurements in the frequency range of $0.01 \leqslant \omega \leqslant 10^7$ Hz were studied using an Alpha-N Analyzer, Novocontrol (Germany). The polarization-electric field loops (P-E loops) were measured on 100 μm thin films by a Precision Premier II Tester (Radiant Technologies, Inc.). The electroding was done using silver paste for the ferroelectric characterization. The energy storage densities of the PVDF-HFP composites were calculated from the electric displacement-electric field curves (D-E loops) by the following equation: $\vec{D} = \varepsilon\vec{E} + \vec{P}$, where E is the applied electric field, P is the polarization and D is the electrical displacement field.

Results and discussion

Morphology of BT and BZT-08 particles

Figure 1 shows the x-ray powder diffraction pattern for $BaTiO_3$ (BT) and $Ba(Ti_{0.92}Zr_{0.08})O_3$ (BZT-08). The inset in these figures show the Bragg profiles of two pseudocubic reflections $\{200\}$[8]$_c$ and $\{103\}_c$, respectively. Pure BT is known to exhibit a tetragonal (P4 mm) structure. The doublet in the $\{200\}_c$ and $\{103\}_c$ reflections, shown in figure 1(a), is characteristic of this tetragonal structure. In comparison, the 8 mol% Zr-modified $BaTiO_3$ seems to exhibit a significantly broader peak due to the appearance of new peaks between the tetragonal peaks. The additional peaks marked with arrows in the insets of figure 1(b) correspond to the orthorhombic phase. This phase, along with the tetragonal phase, gets stabilized at room temperature due to the Zr modification of the BT. The modified compositions have been reported to show enhanced piezoelectric properties [19].

BT and BZT-08 particle-induced structural changes in PVDF-HFP

In order to enhance the dispersion quality of the particles in the composites next to the improved interfacial adhesion with PVDF-HFP, the particles were modified with APTS, as described earlier. Figure 1(c) compares the spectra for silane-modified and unmodified BZT-08 particles. The peaks in the range of 950 – 1250 cm^{-1} represent Si-O-Si vibration modes. Additionally, the peak at 1570 cm^{-1} corresponds to the NH_2 scissoring vibration, thereby confirming the silane molecules on the BZT-08's surface. Similar observations were noted in the case of modified BT particles as well (not shown here). The FTIR scans on the PVDF-HFP and on the composites were also recorded to assess the nature of the interaction between the matrix and the particles (see figure 1(d)). The peaks at 763, 800 and 976 cm^{-1}, which represent the α phase of the PVDF-HFP, are present in both of the composites. Interestingly, the peak at 840 cm^{-1} can only be observed in PVDF-HFP/BT and PVDF-HFP/BZT-08 composites, which strongly suggest the formation of an electroactive β polymorph in the PVDF-HFP. The average particle sizes of

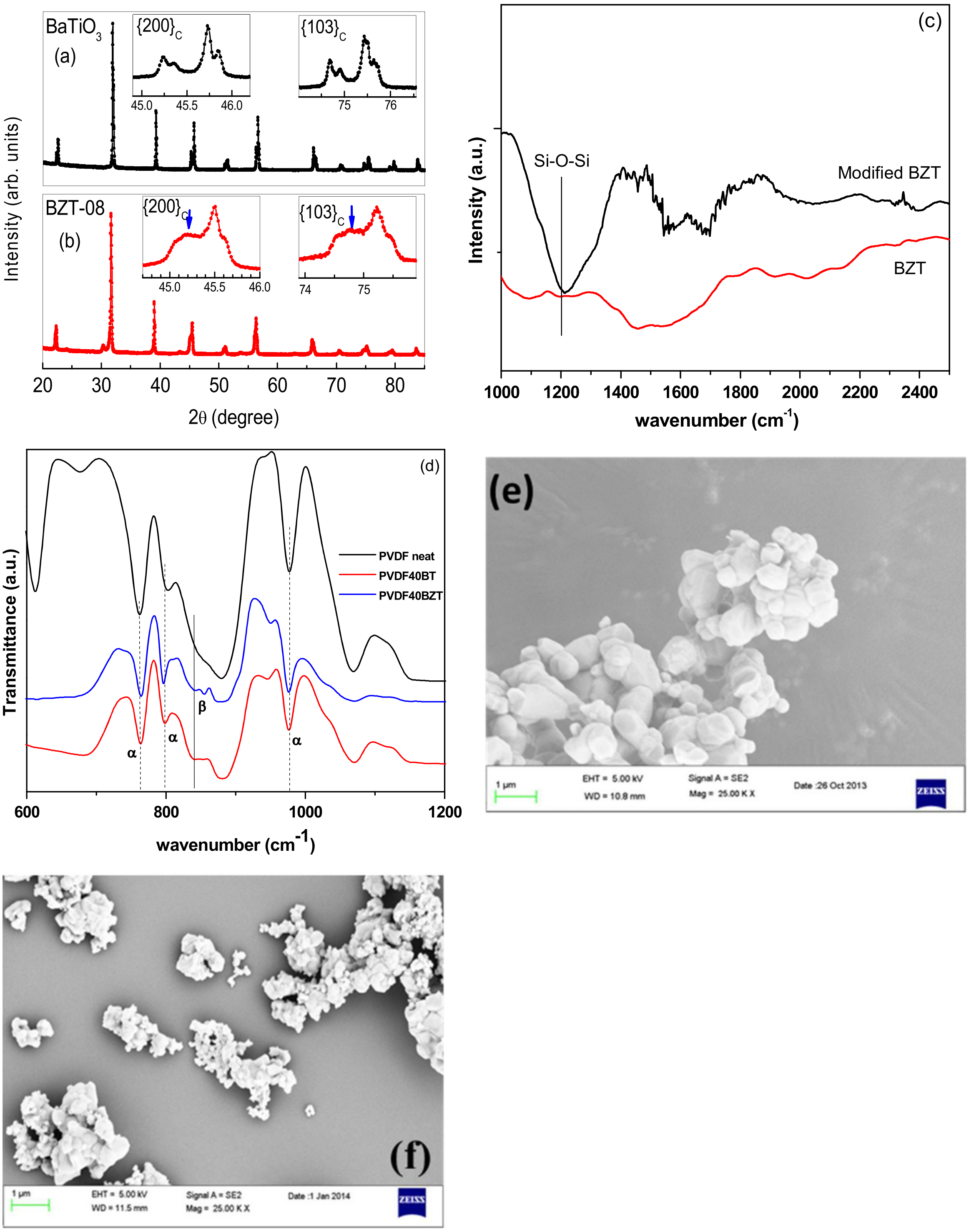

Figure 1. XRD patterns for BT (a) and BZT-08 particles (b), FTIR spectra for PVDF-HFP- and PVDF-HFP-based composites (c), (d), SEM micrographs of modified BT (e) and BZT-08 particles (f), respectively.

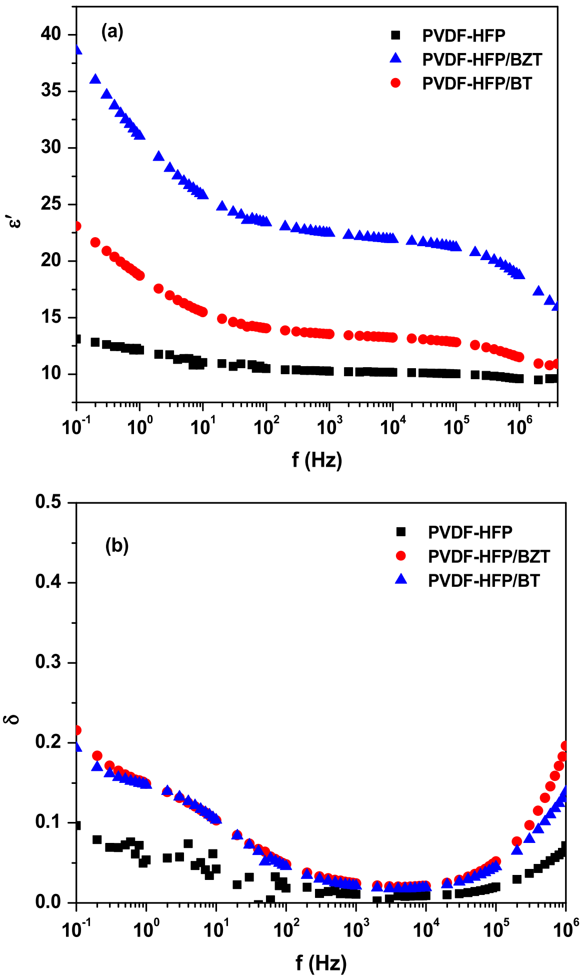

Figure 2. Dielectric constant (a) and tan δ (b) as a function of frequency for PVDF-HFP, PVDF-HFP/BT and PVDF-HFP/BZT-08 composites.

the modified BZT-08 and BT were observed to be 450 nm and 565 nm, respectively, using zeta potential measurements. The corresponding SEM micrographs of the APTS-modified particles are illustrated in figures 1(e), (f). Smaller clusters of the particles are evident, which suggests the key role of the silane coupling agent in modifying the surface of the particle and facilitating the homogeneous dispersion in the composites. Moreover, the average particle sizes obtained from the particle size analyzer corroborate well with the SEM micrographs.

BT and BZT-08-induced electroactive β polymorph in PVDF-HFP: effect on molecular relaxations

Dielectric properties are measured in a broad frequency range, illustrated in figure 2. As a general trend, the dielectric constant of the composites rapidly decreases with the increasing frequency [5], especially in the lower frequencies, and become nearly constant at higher frequencies (see figures 2(a), (b)). From figure 2(a), we can observe that the permittivity in the case of the PVDF-HFP/BZT-08 composites increased due to the addition of the BT particles. For instance, the permittivity of PVDF-HFP is 10.5 at 100 Hz, whereas in PVDF-HFP/BT composites, it increased to 14.5 at 100 Hz. However, the tan delta is only slightly increased with the addition of the BT particles, but the change is not significant (figure 2(b)). The tan delta for the PVDF-HFP is 0.02 at 100 Hz, which is slightly lower in comparison to the PVDF-HFP/BT composites (0.04 at 100 Hz). Further, in PVDF-HFP/BZT-08, the permittivity is increased to 25 at 100 Hz, which is 2.5 times higher in the entire frequency range with respect to the control PVDF-HFP, and it is higher than the PVDF-HFP/BT composites. However, the losses are similar to that observed for PVDF-HFP/BT composites. The increased permittivity in the PVDF-HFP/BZT-08 composites is derived from the enhanced average field in the polymer matrix because of the large difference in the permittivity between the PVDF-HFP and BZT-08. The increased dielectric constant associated with BZT-08 accords well with the β polymorph in the PVDF-HFP.

Enhanced ferroelectric properties in the presence of BZT-08: high remnant polarization

The P-E hysteresis loops of PVDF-HFP- and PVDF-HFP-based composites are displayed in figure 3(a). The introduction of particles appreciably enhances the spontaneous polarization in the composites; interestingly, this polarization is more enhanced in the case of BZT-08 composites. Figure 3(a) depicts the remnant polarization (P_r) as a function of the electric field for neat PVDF-HFP and its composites. The P_r for the PVDF-HFP/BZT-08 composite is observed to be ca. 2.5 μC cm^{-2}, which is significantly higher than that of the control PVDF-HFP (0.7 μC cm^{-2}) and the PVDF-HFP/BT composites (1.6 μC cm^{-2}). With the increase in the electric field, the specimens exhibit higher polarization due to the alignment of the dipoles within the material. Here, the poling at a high temperature contributed significantly toward making the dipoles more flexible. In addition, the presence of ceramic particles facilitated a very high field within the polymer matrix, which resulted in high dielectric permittivity and high P_r. This relatively high response may be due to the stabilization of two ferroelectric phases: tetragonal and orthorhombic, in the case of BZT-08 [10, 11]. Further, open cycle loops manifest in the charge leakage by conduction due to non-infinite resistivity. BT particles generally exhibit a dielectric permittivity of around 1700. Both the piezoelectric and dielectric behavior of BT is greatly improved by Zr modification. The three-phase transformations that occur in BT (T_C, $T_{T\text{-}O}$ and $T_{O\text{-}R}$) are generally characterized by the anomalies in the temperature dependence of the relative permittivity. The stabilization of two ferroelectric phases in the BZT-08 affects the electric polarization dramatically, thereby enhancing the switching and remnant polarization in the composites. Further, the β polymorph in the PVDF-HFP facilitated by the BZT-08 particles advocates the changes in dielectric and ferroelectric properties, resulting in charge accumulation and dipole orientation in the composites. This interfacial charge-trapping at the boundaries of the layers due to non-uniform distribution of the current densities in ceramic particles and in the ferroelectric β phase led to interesting properties in the composites. The particle-matrix interface region exhibits peculiar properties. The increased interface region (as in the case of the composites) significantly influences the overall property of the composites. It is envisaged that all three regions: the continuous matrix phase, the particle and the interface, contribute toward the dielectric properties [14, 20, 22]. In the case of particles, the increased interface results in Maxwell–Wagner–Sillars (MWS) polarization, which emphasizes the role of the diffused Gouy–Chapman layer at the interface leading to the increased polarization of the composite [20, 22]. Hence, such composites can be further explored in energy harvesting applications and as flexible ferroelectric materials.

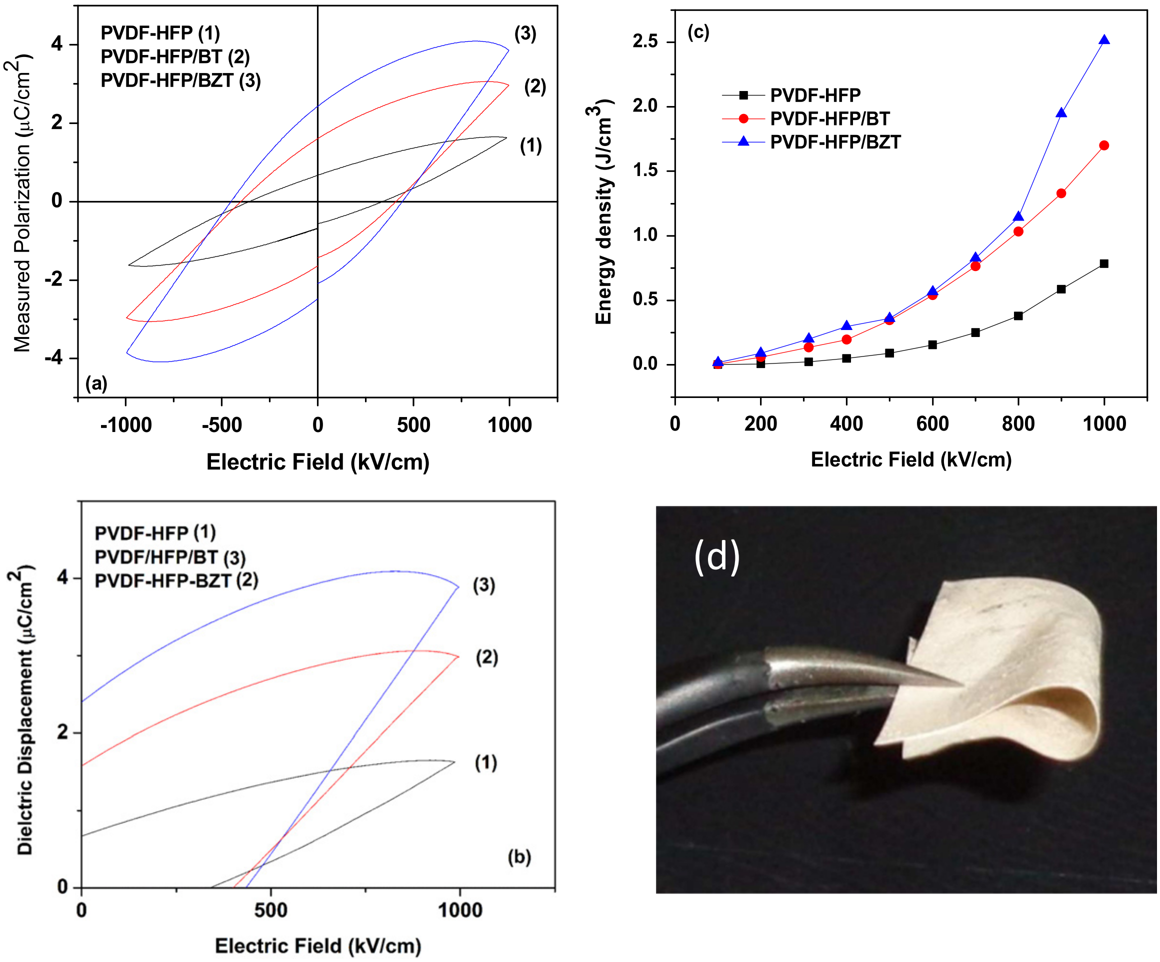

Figure 3. (a) P-E loops for the PVDF-HFP and composites, (b) D-E loops for the PVDF-HFP and the composites as a function of the applied electric field, (c) energy density of the composites as a function of the applied electric field and the (d) flexible PVDF-HFP/BZT-08 composites.

Apart from the ferroelectric properties, the energy storage densities of the PVDF-HFP composites were calculated from the electric displacement-electric field curves (D-E loops) curves by the following equation [18, 22]: $\vec{D} = \varepsilon\vec{E} + \vec{P}$, where E is the applied electric field, P is the polarization and D is the electrical displacement field. The D-E loops of the PVDF-HFP /BZT composites are illustrated in figure 3(b) at 1000 kV cm^{-1}. The electric displacement values increase with the incorporation of BT and BZT at the same electric field (i.e. 1000 kV cm^{-1}) The energy storage densities of the composites are shown in figure 3(c). It is clear that the energy storage density values increase with the incorporation of BT and BZT in the polymer matrix and that this enhancement in the energy density is mainly due to a higher dielectric constant [23]. The PVDF-HFP/BZT composite shows comparatively high energy density value (2.7 J cm^{-3}) as compared to PVDF-HFP/BT (1.6 J cm^{-3}) and PVDF-HFP composites (0.75 J cm^{-3}). Hence, PVDF-HFP/BZT composite can be a potential material for energy storage devices. It is important to note that the reported energy density values were measured on 100 μm thick films, and it is well known that the energy density can be increased by decreasing the film's thickness.

This work further opens new avenues to design materials with a high dielectric constant, low loss and high energy, which can be explored for various applications.

Conclusions

In summary, composites of PVDF-HFP with $BaTiO_3$ (BT) and Zr-modified $BaTiO_3$ (BZT-08) were prepared by melt mixing to design materials with tunable dielectric and ferroelectric properties. For a similar volume fraction, the PVDF-HFP/BZT-08 exhibited much higher ferroelectric properties as compared to the control PVDF-HFP and PVDF-HFP/BT composites. The changes observed in the BZT-08 composites manifested from the stabilization of two ferroelectric phases: tetragonal and orthorhombic, due to high polarization at room temperature. The latter phenomenon also resulted in a higher dielectric as well as a high energy density in the PVDF-HFP/BZT composites, as manifested from the P-E loops.

Acknowledgement

The authors acknowledge the financial support from JATP and DST (India), the spectroscopy and analytical test facility (SID) and the CeNSE characterization facility (MNCF) at IISc.

References

[1] Barber P, Balasubramanian S, Anguchamy Y, Gong S, Wibowo A, Gao H, Ploehn H and Zur Loye H-C 2009 Polymer composite and nanocomposite dielectric materials for pulse power energy storage *Materials* **2** 1697–733

[2] Bose S and Mahanwar P A 2005 Influence of particle size and particle size distribution on MICA filled nylon 6 composite *J. Mater. Sci.* **40** 6423–8

[3] Bose S, Raghu H and Mahanwar P A 2006 Mica reinforced nylon-6: effect of coupling agents on mechanical, thermal, and dielectric properties *J. Appl. Polym. Sci.* **100** 4074–81

[4] Cauda V, Stassi S, Bejtka K and Canavese G 2013 Nanoconfinement: an effective way to enhance PVDF piezoelectric properties *ACS Appl. Mater. Interfaces* **5** 6430–7

[5] Chanmal C V and Jog J P 2008 Dielectric relaxations in PVDF/$BaTiO_3$ nanocomposites *Express Polym. Lett.* **2** 294–301

[6] Dang Z-M, Wang H-Y and Xu H-P 2006 Influence of silane coupling agent on morphology and dielectric property in $BaTiO_3$/polyvinylidene fluoride composites *Appl. Phys. Lett.* **89** 112902

[7] Ertuğ B 2013 The overview of the electrical properties of barium titanate *Am. J. Eng. Res.* **2** 01–07

[8] Gregorio R Jr, Cestari M and Bernardino F 1996 Dielectric behaviour of thin films of β-PVDF/PZT and β-PVDF/$BaTiO_3$ composites *J. Mater. Sci.* **31** 2925–30

[9] Iijima M, Sato N, Wuled Lenggoro I and Kamiya H 2009 Surface modification of $BaTiO_3$ particles by silane coupling agents in different solvents and their effect on dielectric properties of $BaTiO_3$/epoxy composites *Colloids Surf.* A **352** 88–93

[10] Kalyani A K and Ranjan R 2013 Anomalous piezoelectric response due to stabilization of two ferroelectric phases in Zr-modified $BaTiO_3$ *J. Phys.: Condens. Matter.* **25** 362203

[11] Kalyani A K, Senyshyn A and Ranjan R 2013 Polymorphic phase boundaries and enhanced piezoelectric response in extended composition range in the lead free ferroelectric $BaTi_{1-x}Zr_xO_3$ *J. Appl. Phys.* **114**

[12] Kim P, Jones S C, Hotchkiss P J, Haddock J N, Kippelen B, Marder S R and Perry J W 2007 Phosphonic acid-modified barium titanate polymer nanocomposites with high permittivity and dielectric strength *Adv. Mater.* **19** 1001–5

[13] Li Y, Huang X, Hu Z, Jiang P, Li S and Tanaka T 2011 Large dielectric constant and high thermal conductivity in poly(vinylidene fluoride)/barium titanate/silicon carbide three-phase nanocomposites *ACS Appl. Mater. Interfaces* **3** 4396–403

[14] Lin M-F and Lee P S 2013 Formation of PVDF-g-HEMA/BaTiO3 nanocomposites via *in situ* nanoparticle synthesis for high performance capacitor applications *J. Mater. Chem.* A **1** 14455–9

[15] Muralidhar C and Pillai P 1987 Dielectric behaviour of barium titanate ($BaTiO_3$)/polyvinylidene fluoride (PVDF) composite *J. Mater. Sci. Lett.* **6** 346–8

[16] Muralidhar C and Pillai P 1988 Dielectric behaviour of barium titanate-polyvinylidene fluoride composites *J. Mater. Sci.* **23** 1071–6

[17] Patsidis A and Psarras G C 2008 Dielectric behaviour and functionality of polymer matrix–ceramic $BaTiO_3$ composites *Express Polym. Lett.* **2** 10

[18] Sharma M, Madras G and Bose S 2014 Process induced electroactive β-polymorph in PVDF: effect on dielectric and ferroelectric properties *Phys. Chem. Chem. Phys.* **16** 14792–9

[19] Song Y, Shen Y, Liu H, Lin Y, Li M and Nan C-W 2012 Improving the dielectric constants and breakdown strength of polymer composites: effects of the shape of the $BaTiO_3$ nanoinclusions, surface modification and polymer matrix *J. Mater. Chem.* **22** 16491–8

[20] Todd M G and Shi F G 2005 Complex permittivity of composite systems: a comprehensive interphase approach *IEEE Trans. Dielectr. Electr. Insul.* **12** 601–11

[21] Nguyen V S, Rouxel D, Meier M, Vincent B, Dahoun A, Thomas S and Dos Santos F D 2014 Effect of ultrasonication and other processing conditions on the morphology, thermomechanical, and piezoelectric properties of poly(vinylidene difluoride-trifluoroethylene) copolymer films *Polym. Eng. Sci.* **54** 1280–8

[22] Wang Q and Zhu L 2011 Polymer nanocomposites for electrical energy storage *J. Polym. Sci. Part B: Polymer Physics* **49** 1421–9

[23] Xie L, Huang X, Yang K, Li S and Jiang P 2014 'Grafting to' route to PVDF-HFP-GMA/$BaTiO_3$ nanocomposites with high dielectric constant and high thermal conductivity for energy storage and thermal management application *J. Mater. Chem.* A **2** 5244–51

[24] Zhu L and Wang Q 2012 Novel ferroelectric polymers for high energy density and low loss dielectrics *Macromolecules* **45** 2937–54